Glutamatergic transmission and plasticity between olfactory bulb mitral cells

Diogo O. Pimentel and Troy W. Margrie

The Department of Neuroscience, Physiology and Pharmacology, University College London, Gower Street, London WC1E 6BT, UK

In the olfactory bulb the sets of mitral cells that project their apical dendrite to the same glomerulus represent unique functional networks. While it is known that mitral cells release vesicular glutamate from their apical tuft it is believed that the resultant self-excitation (SE), transmitted via dendritic gap junctions, is the main form of lateral transmission within the mitral cell assembly. In this study we used simultaneous whole-cell recordings from mitral cell pairs to show that a direct form of chemical lateral excitation (LE) provides a means of mitral cell–mitral cell communication. In contrast to the ubiquitous expression and robust nature of SE, the efficacy of glutamatergic LE between mitral cells is highly variable and mediated by calcium-impermeable AMPA receptors. We also find that the strength of LE is bi-directionally modulated, in a homeostatic manner, by sniffing-like patterns of presynaptic activity. Since these changes last many minutes we suggest that such mitral cell–mitral cell interactions provide the glomerular network with a locus for olfactory plasticity and a potential mechanism for receptive field modulation.

Across the surface of the olfactory bulb each glomerulus receives specified inputs from the nose that are integrated by a dedicated ensemble of 50–100 principal mitral and tufted cells. While it is generally agreed that the release of vesicular glutamate from mitral cell dendrites onto local inhibitory interneurons provides a mechanism for recurrent and centre-surround inhibition in the bulb (Pinching & Powell, 1971*a*; Jahr & Nicoll, 1980; Aungst *et al.* 2003; Murphy *et al.* 2005) it is not known how mitral–mitral cell interactions contribute to such processes. Determining whether discharge of an individual mitral cell directly impacts on the excitability of the glomerular mitral cell assembly, will therefore enhance our understanding of the mechanisms of sensory representation within and across such functional modules.

In addition to evoking recurrent and lateral inhibition, the release of glutamate from mitral cell dendrites is also known to evoke both AMPA and NMDA receptor-mediated potentials in the same cell, resulting in a direct form of recurrent self-excitation (SE) (Nicoll & Jahr, 1982; Isaacson, 1999; Margrie *et al.* 2001; Salin *et al.* 2001; Schoppa & Westbrook, 2001, 2002). Simultaneous recordings from intraglomerular pairs of mitral cells also show EPSP-like depolarizations in the second cell (Schoppa & Westbrook, 2002; Urban & Sakmann, 2002; Christie & Westbrook, 2006). Gap junctions located in the tuft, proximal to the source of self excitation (Salin

et al. 2001) are thought to electrically transmit EPSP-like depolarizations through the mitral cell network (Schoppa & Westbrook, 2002; Christie *et al.* 2005; Christie & Westbrook, 2006). Due to a lack of electron micrographic evidence in support of mitral cell–mitral cell synapses (Price & Powell, 1970; Pinching & Powell, 1971*b*; Kosaka & Kosaka, 2005), lateral transmission is thought to be due solely to gap junction-mediated electrical transfer of SE (Schoppa & Westbrook, 2001, 2002; Christie *et al.* 2005; Christie & Westbrook, 2006). While this form of electrically mediated lateral transmission has been shown to facilitate spike synchronization across the glomerular network (Schoppa & Westbrook, 2001, 2002; Christie *et al.* 2005; Christie & Westbrook, 2006) the precise relationship between SE, electrical coupling and lateral communication between mitral cells is not understood. To date it is assumed that any chemical form of lateral transmission between intraglomerular mitral cells can only occur under conditions that produce non-physiologically elevated levels of glutamate (Schoppa & Westbrook, 2001, 2002; Christie *et al.* 2005; Christie & Westbrook, 2006).

Plasticity within olfactory bulb dendro-dendritic networks has long been proposed to provide a mechanism for olfactory memory (Rosser & Keverne, 1985; Kaba & Keverne, 1988; Sullivan *et al.* 2000), sensory adaptation (Li, 1990), tuning receptive fields and even discrimination learning (Wilson *et al.* 2004). Despite these proposed

benefits, evidence for neuronal plasticity between dendritic connections in the bulb or for dendritic transmission in general has not been forthcoming. This raises questions as to whether or not dendritic transmission is functionally more hard-wired than axonal transmission and whether or not dendro-dendritic transmission in the olfactory bulb can provide the kind of activity-dependent plasticity observed at many axo-dendritic synapses.

Here we explore directly the relationship between SE, electrical coupling and lateral transmission within intraglomerular mitral cell networks. We show that in addition to electrical coupling, chemical lateral transmission provides a second form of mitral cell–mitral cell communication. The efficacy of this form of dendritic transmission is variable but independent of the strength of electrical coupling and the degree of SE observed in the presynaptic cell. In contrast to SE, glutamatergic lateral excitation (LE) is not ubiquitous and does not rely on calcium-permeable AMPA receptors. Furthermore, and in contrast to electrical transmission, LE provides a dedicated excitatory loop throughout the mitral cell network that is bi-directionally modulated by sniffing-like patterns of mitral cell activity.

Methods

All procedures and animal handling were performed according to the UK Animals (Scientific Procedures) Act 1986. C57BL/6 P20–P27 mice were decapitated and horizontal olfactory bulb slices ($300\,\mu m$ thick) were prepared and maintained in 'low calcium' aCSF (mM: NaCl 125; KCl 2.5; $NaHCO_3$ 26; $NaH_2PO_4.H_2O$ 12.5; $CaCl_2$ 1; $MgCl_2$ 2; glucose 25) equilibrated with 95% O_2–5% CO_2. Whole-cell recordings were performed from the somas of visually identified mitral and tufted cells using infrared differential interference contrast (IR-DIC) microscopy. Electrodes (4–$7\,M\Omega$ resistance) were filled with a low chloride internal solution containing (mM): methansulphonic acid 130; Hepes 10; KCl 7; EGTA 0.05 Na_2ATP 2; MgATP 2; Na_2GTP 0.5; biocytin 0.4%; titrated to pH 7.4 with 1 M KOH. The extracellular solution contained (mM): NaCl 125; KCl 2.5; $NaHCO_3$ 26; $NaH_2PO_4.H_2O$ 12.5; $CaCl_2$ 2; $MgCl_2$ 1; glucose 26, equilibrated with 95% O_2-5% CO_2 plus $50\,\mu M$ picrotoxin (unless stated otherwise). Ionotropic glutamate receptor blockers were applied at the following concentrations: AP-V (R-2-amino-5-phosphonopentanoate) $25\,\mu M$; NBQX (3-dihydroxy-6-nitro-7-sulfamoyl-benzo(f)quinoxaline) 10–$20\,\mu M$; NAS (naphthyl-acethyl-spermine) $20\,\mu M$. Whole-cell recordings were obtained using a Multiclamp 700B amplifier, filtered at 6–10 kHz and digitized at 10–20 kHz using an ITC-18 data acquisition board controlled by the Nclamp/Neuromatic package. Data were analysed using Neuromatic (www.neuromatic. thinkrandom.com) software that runs within the Igor Pro (Wavemetrics) environment.

For both SE and LE experiments, action potentials (APs) were evoked by injecting current pulses of 2 ms duration and 1.6–1.8 nA in amplitude. Reported measurements of the strength and monitoring of SE and LE refer to responses evoked by a single AP (except for the quantification of paired-pulse responses). The peak time was determined from an average of at least 12 sweeps and defined as the time at which the membrane voltage reaches the maximum within a 10 ms interval beginning 0.5 ms after the end of the 'presynaptic' current injection. A 2 ms averaging window was centred around the peak time and compared with a 2 ms baseline window that ended 1 ms before the beginning of the presynaptic current injection time. The difference in membrane voltage between the two windows was quantified as being the amount of SE or LE. In cases where LE was smaller than 0.2 mV the peak depolarization values from at least 12 individual sweeps were statistically compared with those from the baseline window. In cases in which the membrane voltage in the second cell was not statistically different from the baseline value, LE was considered to be not detectable. To minimize contamination by voltage-dependent conductances, SE was determined by digitally subtracting the action potential waveforms in the presence of AMPA receptors antagonists from the control waveforms in traces in which the baseline membrane voltage differed by less than $300\,\mu V$. Paired-pulse ratios were quantified by dividing the amplitude of the second EPSP by the first, evoked by two APs at 20 Hz. Theta burst stimulation (TBS) consisted of 150 bursts of five APs at 50 Hz repeated at 5 Hz (750 APs, total duration 30 s). Recurrent inhibitory postsynaptic potentials were evoked using a burst of five APs at 50 Hz and determined by digitally subtracting the burst waveforms in the presence of picrotoxin from those under control conditions (Margrie *et al.* 2001). Similarly recurrent IPSP amplitude was quantified as the difference between a 2 ms baseline window positioned before the first AP and a 2 ms detection window which was set centred around the minimum voltage of the subtracted waveform.

Gap junction coupling was assessed by injection of hyperpolarizing pulses (-400 to -800 pA, 600 ms duration) alternating to both cells. Electrical coupling was quantified by determining the ratio (coupling coefficient) between the steady state amplitude of the evoked voltage deflection in the test cell to the response evoked in the presynaptic cell. In cases where the average coupling coefficient for both directions was smaller than 0.01 the postsynaptic hyperpolarizations were checked for statistical significance. In all cases where the morphology of pairs could be confirmed, mitral cells projecting to the same glomerulus showed statistically significant coupling coefficients. The same pulses were used to monitor input resistance during the plasticity experiments.

Dendrotomies were carried out either indirectly (via non-specific amputation during the slicing procedure) or directly using two patch pipettes in a scissor-like motion under visual guidance. In all cases dendritic amputation was confirmed by morphological analysis. Recovery of biocytin-filled cells was carried out as previously described (Horikawa & Armstrong, 1988) and cells were reconstructed using the Neurolucida system (Microbrightfield Inc.). Quantification of mitral cell morphometric properties was performed using the built-in analysis functions of Neurolucida Explorer (integrant part of the Neurolucida System; Micro-brightfield Inc.). For the quantification of mitral cell tuft morphology the soma, apical dendrite and lateral dendrites were not considered. For the quantification of lateral dendrites the soma and apical dendrite were excluded. Surface area was computed by treating dentritic segments as frusta. The three-dimensional Convex Hull analysis provides an estimate of the size of the dendritic field of the tufts. It is derived from a convex polygon generated by connecting the tips of the outer dendritic processes. The surface area of the smallest convex polygon for both tufts therefore provides a measure of the space occupied within a glomerulus. For determining the predicted mean surface area for a mitral cell pair, 12 single mitral cells (i.e. cells projecting to different glomeruli, i.e. non-pairs) were reconstructed and their morphologies quantified. Mean values were calculated and multiplied by a factor of two and used as the expected pair morphometry. For the dendritic proximity analysis, histograms reflecting the distance between dendrites belonging to different cells were obtained from Neurolucida Explorer. The minimum distance (or dendritic proximity) was considered to be the lower limit of the first bin (each bin $0.1\,\mu$m wide) containing data points.

In several instances displaced mitral cells/tufted cells (whose somas where no more than $166\,\mu$m distant from the mitral cell layer) were also recorded from in this study (7 tufted cells out of 198 total cells; no simultaneous recordings from 2 tufted cells are included). Within this subgroup we found representatives of all the functional groups (4 uni-directional, 2 bi-directional and 1 neither direction). We found no significant difference between the amplitude of lateral transmission in tufted cell-containing pairs when compared with the remaining population (tufted cell-containing pairs 0.42 ± 0.26 mV, $n = 6$ connections *versus* exclusively mitral cell pairs 0.53 ± 0.54 mV, $n = 117$ connections; $P > 0.05$). Furthermore no significant difference was found in the average tuft morphology (tufted cell-containing pairs: average tuft surface area $6349 \pm 2970\,\mu$m^2 and 67 ± 36 nodes *versus* exclusively mitral cell pairs $8017 \pm 2599\,\mu$m^2 and 90 ± 27 nodes; $P > 0.05$). Given these data these cells have been pooled and the general term mitral cell been used. This does not mean to imply that there are not potentially other functional differences between these two cell types (Haberly & Price, 1977; Mori *et al.* 1983; Hayar *et al.* 2004; Nagayama *et al.* 2004; Hayar *et al.* 2005; Karnup *et al.* 2006).

Results

It has been shown that a single action potential in a mitral cell can evoke an EPSP-like depolarization in an intraglomerular partner (Fig. 1*A*, top) that is sensitive to
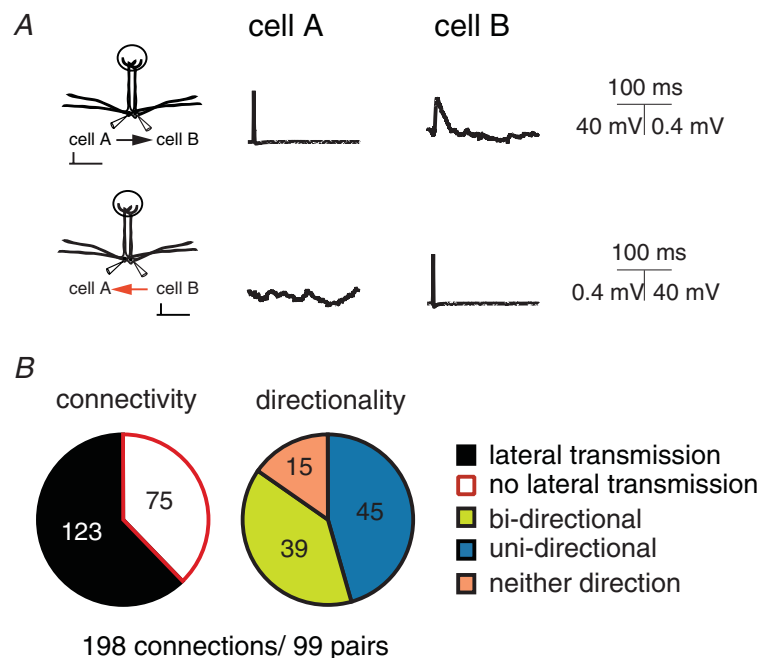

Figure 1. Connectivity and directionality of lateral transmission between mitral cells
A (top), example recordings performed in current clamp from a pair of mitral cells projecting to the same glomerulus. Evoking a single AP in cell A (top left) can result in a detectable depolarization in cell B (top right). For the same pair an AP in cell B failed to evoke detectable lateral transmission (bottom). *B*, pie charts showing the overall connectivity and directionality of lateral transmission across 99 pairs of mitral cells (198 possible connections).

blockers of the AMPA and NMDA subtypes of ionotropic glutamate receptors (Schoppa & Westbrook, 2002; Urban & Sakmann, 2002; Christie & Westbrook, 2006). This phenomenon has been interpreted as lateral transmission of self excitation via gap junctions (Schoppa & Westbrook, 2002). Using simultaneous whole-cell recordings (in the presence of picrotoxin) from pairs of mitral cells (i.e. mitral cells that project their apical dendrites to the same glomerulus; $n = 99$) we find that although lateral transmission is observed in the majority of cases (Fig. 1*B*, top; average amplitude 0.53 ± 0.05 mV $n = 123$ connections) it is not a universal feature of intra-glomerular mitral–mitral cell communication (absent in 75/198 potential conections, Fig. 1*B*). Therefore we sorted pairs into three possible categories according to the expression of lateral transmission: those that expressed lateral transmission in both connections (bi-directional 39/99 pairs; Fig. 1*B* right, green), in a single connection (uni-directional 45/99 pairs; Fig. 1*B* right, blue) or neither of the possible directions (neither direction 15/99 pairs; Fig. 1*B* right, orange). In all the cases where lateral transmission was not observed, the co-localization of mitral cell tufts to the same glomerulus was confirmed either anatomically ($n = 6$) or by the existence of electrical coupling ($n = 9$).

Since the existence and strength of lateral transmission varied considerably between mitral cell pairs one obvious explanation might be that its extent and efficacy varies with intactness of the apical tuft/s which might be compromised by the slicing procedure. We therefore compared the amplitude of lateral transmission between randomly selected pairs ($n = 18$) to several morphometric parameters including the number of branch points, total membrane surface area and the convex Hull surface – a measure of the space occupied by the two dendritic tufts. This morphological data set was then separated into the categories bi-directional, uni-directional or neither, based on the existence and directionality of lateral transmission (Fig. 2*A* and *B*).

Analysis of variance revealed no relationship between the incidence of lateral transmission and the pair tufts macroscopic features (branch points $F_{(2,15)} = 0.97$, $P > 0.4$; tuft surface area $F_{(2,15)} = 0.99$, $P > 0.3$; convex Hull surface $F_{(2,15)} = 0.27$, $P > 0.7$). There was also no correlation between lateral transmission amplitude and the number of branch points ($R^2 = 0.001$, $P > 0.9$), tuft surface area ($R^2 = 0.059$, $P > 0.3$) or convex Hull surface area ($R^2 = 0.003$, $P > 0.7$; Fig. 2*A* and *Ba–c*). Furthermore, the mean number of branch points and membrane surface area of the 18 reconstructed pairs did not differ from morphological data obtained from individual, non-paired mitral cells (Fig. 2*C*; $P > 0.05$). One explanation for lack of correlation between tuft morphometry and the expression and amplitude of lateral transmission could be that, despite being exclusive to intraglomerular pairs, lateral trans-mission does not occur within the apical tuft but rather via the lateral dendrites. In order to address this notion, we also reconstructed the lateral dendrites of a subset of the previously analysed pairs ($n = 5$) that showed lateral trans-mission in at least one direction and a mean amplitude identical to that of the recorded population (Fig. 2*Da* and *b*). We found that, in contrast to the tuft where dendritic processes are often in very close opposition (mean minimum distance $0.32 \pm 0.07\ \mu$m, $n = 5$), lateral dendrites were typically far more distant (closest distance ranging from 1 to $6.5\ \mu$m; mean minimum distance $2.98 \pm 1.99\ \mu$m, $n = 5$). Taken together these data suggest that although the anatomical locus of lateral transmission is likely within the glomerulus, the observed variability in the incidence, directionality and amplitude of lateral transmission does not result from variable amputation of dendritic tufts due to the slicing procedure or naturally occurring morphological differences.

The role of gap junction-mediated coupling and self-excitation in lateral transmission

In no cases have we observed electrical coupling between simultaneously recorded mitral cells whose apical dendritic tufts belonged to different glomeruli (i.e. non-pairs; $n = 14/14$). In contrast, in all cases where gap junction coupling was observed and histological recovery carried out, we observed a perfect correspondence between coupling and the glomerular location of the dendritic tufts (Fig. 3*A* and *B*; $n = 133$; Schoppa & Westbrook, 2002; Christie *et al.* 2005; Christie & Westbrook, 2006). Since lateral transmission between mitral cells is proposed to be due to the propagation of SE via gap junction-mediated electrical coupling we next investigated directly the relationship between the degree of electrical coupling and the strength of lateral transmission. Under physiological conditions we found that the degree of gap junction coupling between pairs of mitral cells projecting to the same glomerulus (Schoppa & Westbrook, 2002) did not predict the strength nor the likelihood of expression of lateral transmission ($R^2 = 0.002$, $P > 0.5$, $n = 128$; Fig. 3*C*).

One obvious potential explanation for the lack of correlation between electrical coupling and lateral trans-mission is that SE is in general quite potent but variable and that the amplitude of SE via gap junctions largely determines the extent of lateral transmission. Firstly, by comparing SE amplitude in cells with intact dendritic tufts to those in which the apical dendrite had been amputated (Fig. 4*A*) it is evident that the anatomical locus for SE in the mouse, as in the rat, is largely the apical dendritic tuft (Fig. 4*Ba* and *b*; Salin *et al.* 2001). Without exception SE was observed in mitral cells with an

intact tuft, ranging in amplitude from 0.62 mV to 8.5 mV (average 2.04 ± 0.31 mV, 28/28 cells; Fig. 4*Ba* left and *Bb*, filled bars). In contrast, all recorded dendrotomised cells lacked SE (average 0.03 ± 0.05 mV, $n = 5/5$; Fig. 4*Ba* right,

and Fig. 4*Bb*, open bar). One further possibility, however, is that dendrotomy leads to a general degradation in the release machinery within apical and lateral dendrites. To assess this possibility we also investigated the effect of
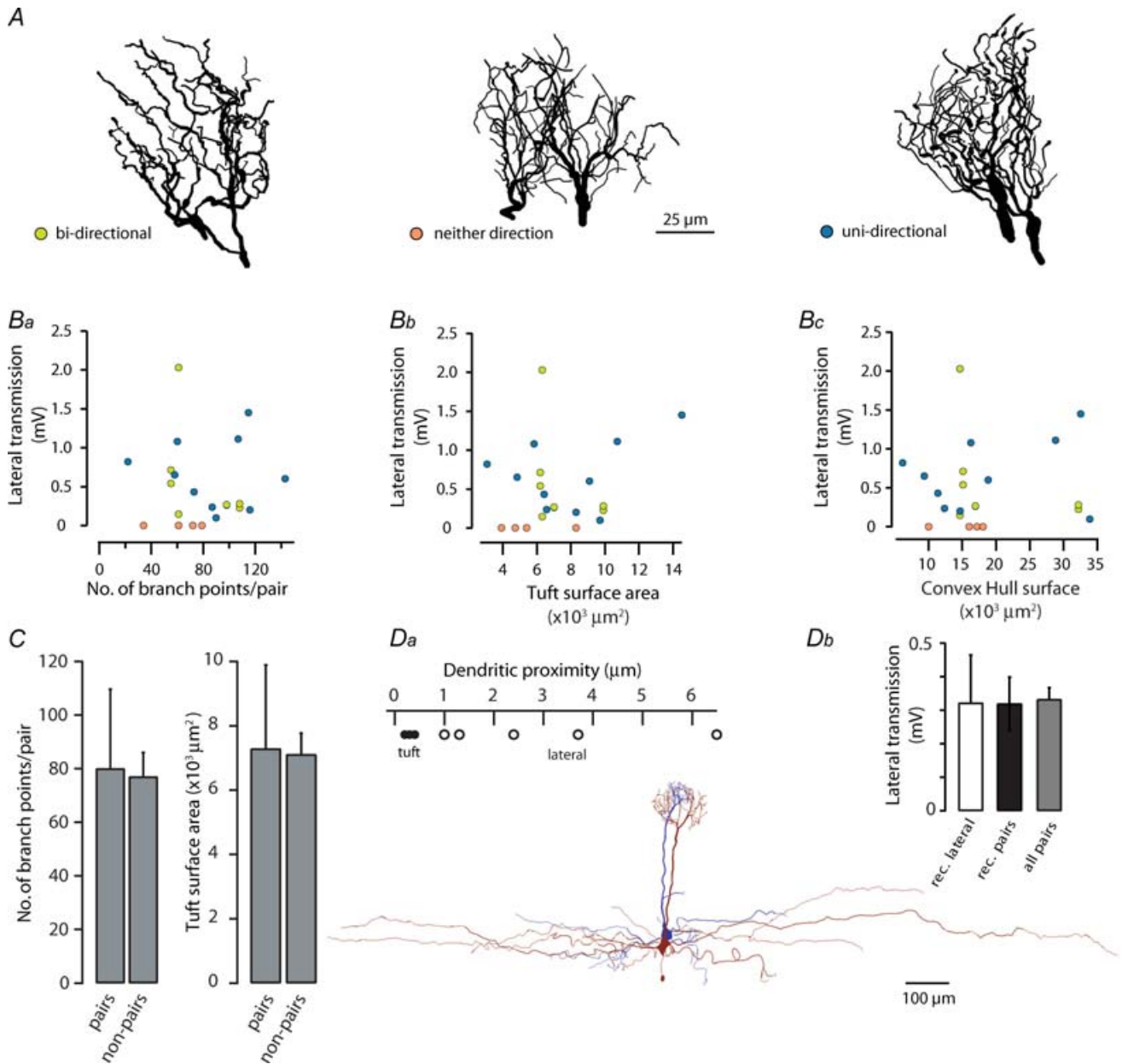

Figure 2. The efficacy and occurrence of lateral transmission does not correlate with tuft morphology
A, example Neurolucida reconstructions of pairs of dendritic tufts for each of the three lateral transmission directional groupings. *B*, graphs showing the relationship between the total number of branch points (*Ba*), surface area (*Bb*) and convex Hull surface (*Bc*) and the amplitude of lateral transmission (bi-directional (both directions plotted), $n = 8$ connections (green circles); uni-directional (a single direction plotted), $n = 10$ (blue circles); neither direction (a single direction plotted), $n = 4$ (orange circles); total, $n = 22$ connections from 18 pairs). *C*, comparison of the average morphometric properties of both reconstructed tufts per pair ($n = 18$ pairs) to those from individual cells that did not project their apical dendrites to the same glomerulus (non-pairs; $n = 12$ cells, each tuft multiplied by a factor of 2; error bars correspond to standard deviation). *D*, in a subset of pairs lateral dendrites ($n = 5$) were also reconstructed (inset bottom). *Da*, a plot showing the minimum distance bin (bins were 0.1 μm wide; lower bin limit plotted – see Methods) obtained from a histogram of dendritic distances (●, apical tuft; ○, lateral dendrites). *Db*, a plot showing the amplitude of lateral transmission for pairs where lateral dendrites were reconstructed (rec. laterals, $n = 5$ pairs), all pairs where the tufts were reconstructed (rec. pairs $n = 18$ pairs) and for the entire data set (all pairs, $n = 99$ pairs; bars correspond to standard error).

dendrotomy on the recurrent IPSP that, at least in part, will be evoked by glutamate release from mitral cell lateral dendrites (Rall *et al.* 1966; Jahr & Nicoll, 1982; Margrie *et al.* 2001). We find that, in contrast to SE, recurrent inhibition is not impaired in dendrotomised cells (Fig. 4*C*, intact 2.46 ± 1.28 mV $n = 5$; dendrotomised 6.52 ± 6.11 mV, $P > 0.05$ Mann–Whitney test; $n = 5$). Though not significant, the apparent trend towards an increase in recurrent inhibition could be explained by an increase in input resistance for dendrotomised cells (Fig. 4*C*, intact 47.4 ± 20.3 MΩ, $n = 7$ *versus* dendrotomised 75.8 ± 17.0 MΩ, $n = 7$,

$P < 0.05$ Mann–Whitney test; (Bekkers & Hausser, 2007). Taken together, our dendrotomy data indicate that SE is a universal feature of mitral cell excitability and occurs primarily in the apical tuft, providing an ideal source for electrical transmission of glutamate receptor-mediated depolarizations within intraglomerular networks.

If SE is the primary source of lateral transmission then together with the coupling coefficient of a given pair it should correlate with the amplitude of lateral transmission between mitral cells (Schoppa & Westbrook, 2002). Where possible we therefore quantified SE, the
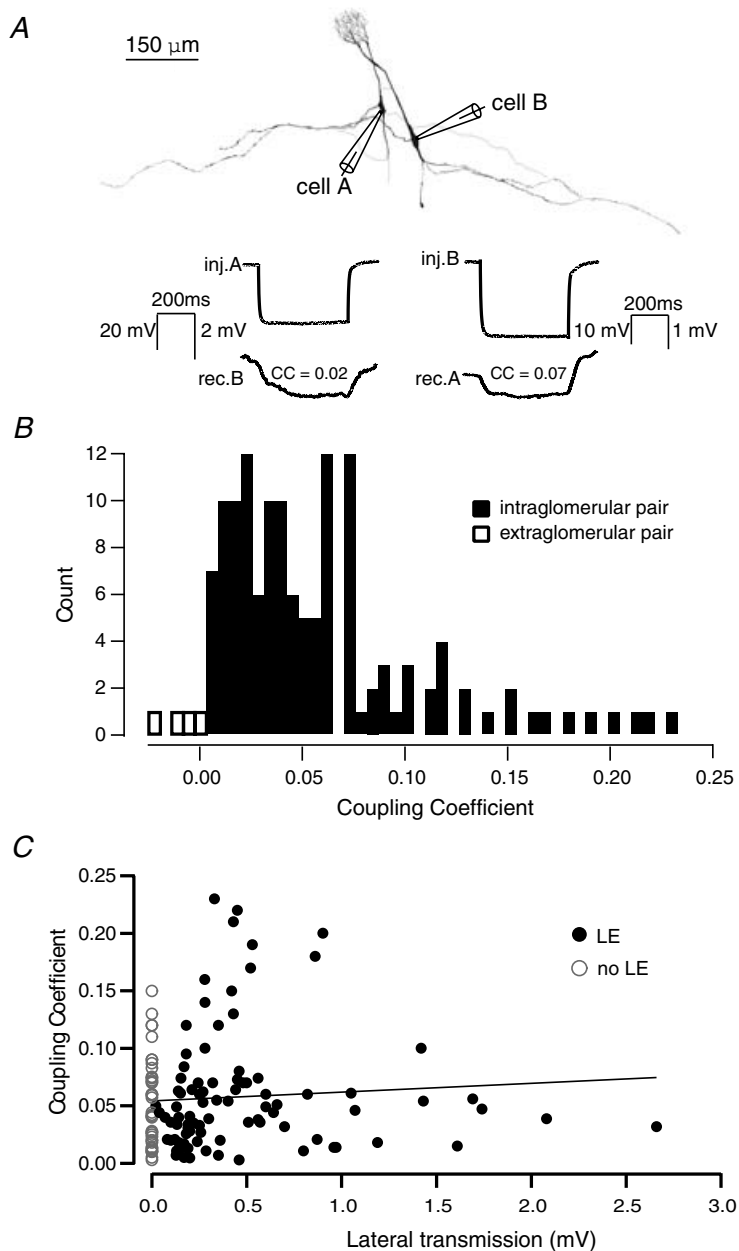

Figure 3. Electrical coupling is ubiquitous and reciprocal among intraglomerular mitral cells
A (top), example reconstructions of a morphologically defined pair of mitral cells. Bottom, example average traces (20 sweeps) recorded in current clamp showing bi-directional electrical coupling assessed by hyperpolarizing pulses in each cell. *B*, histogram showing the distribution of coupling coefficients for 133 connections (filled bars) and 4 non-pairs (open bars). *C*, plot showing the lack of correlation between electrical coupling and lateral transmission.

coupling coefficients and lateral transmission for the same mitral–mitral cell connections ($n = 10$; Fig. 5). While some connections showed a modest amount of SE and coupling with robust lateral transmission, others showed small or no detectable lateral transmission despite similar degrees of coupling and moderate SE. Overall we found no correlation between SE, the degree of coupling and lateral transmission (Fig. 5, $R^2 = 0.11$ $P > 0.3$, $n = 10$). This lack of correlation hints at the existence of an alternative form of transmission between mitral cells.

Self-excitation and lateral transmission are distinct forms of mitral cell signalling

Recent studies indicate that both calcium-permeable and calcium-impermeable AMPA receptors co-exist within
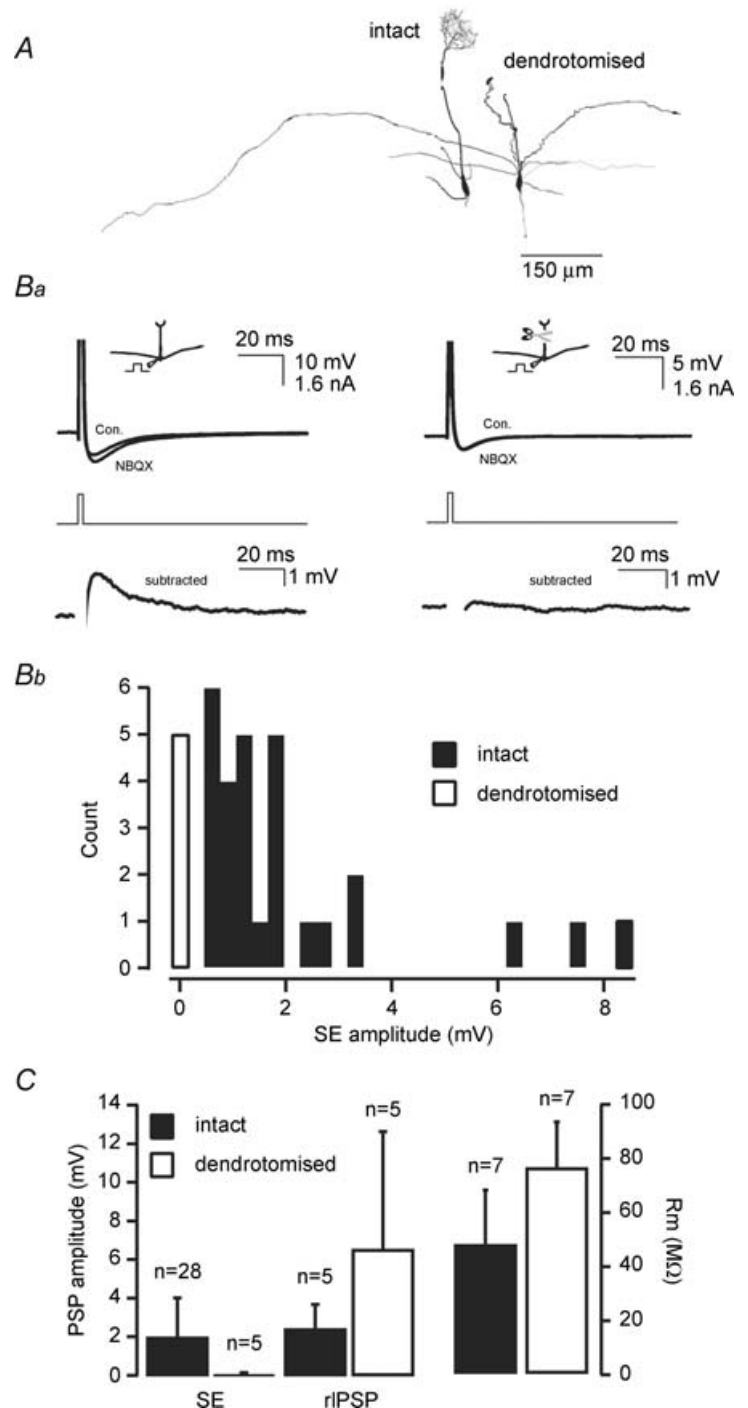

Figure 4. Self-excitation is expressed in all intact mitral cells
A, Neurolucida reconstructions of examples of an intact and a dendrotomised mitral cell. *Ba*, digital subtraction of average AP waveforms (30 sweeps) recorded in current clamp in the absence and presence of NBQX (10 μM) for intact and apically dendrotomised mitral cells. *Bb*, amplitude distribution of SE in intact (filled bars, $n = 28/28$) and dendrotomised cells (open bars, $n = 5/5$). *C* (left), plot comparing the amplitude of self-excitation and recurrent inhibition (rIPSP) and the input resistance for intact cells and dendrotomised cells. Resting membrane potential was -55.0 ± 4.9 mV (control, $n = 5$) and -51.4 ± 3.0 mV (dendrotomised, $n = 5$; $P > 0.05$ Mann–Whitney test; bars correspond to standard deviation).
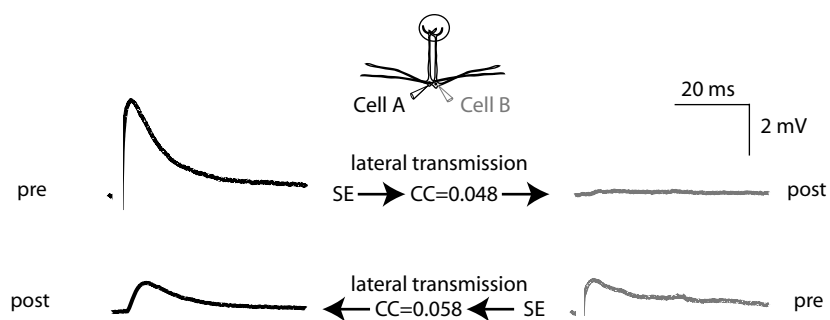
Figure 5. Expression of self excitation and lateral transmission
Example traces (15 sweeps) from a simultaneously recorded pair of cells in which SE, the coupling coefficient and lateral transmission were determined for both directions. In one direction (cell A→cell B; top) large SE (3.60 mV) was observed which resulted in modest lateral transmission (0.15 mV). In contrast, in the other direction (cell B→cell A; bottom) we observed lateral transmission (1.05 mV) that was similar in amplitude to the observed SE in cell B (1.13 mV).

olfactory bulb glomeruli (Montague & Greer, 1999; Blakemore *et al.* 2006; Ma & Lowe, 2007). In order to potentially dissect SE and lateral transmission we examined whether SE and lateral transmission relied on different types of AMPA receptors. We found that bath application of the specific calcium-permeable AMPA receptor antagonist naphthyl-acethyl-spermine (NAS, 20 μM) blocked SE by approximately 71% (residual was $28.6 \pm 21.3\%$ of control amplitude $n = 8$, $P < 0.01$ Wilcoxon paired sample test; Fig. 6*A*). In contrast NAS had little effect on lateral transmission ($80.8 \pm 21.4\%$ of control amplitude $n = 7$, $P > 0.05$ Wilcoxon paired sample test; Fig. 6*B*). These experiments confirm that SE within and lateral transmission between mitral cells are predominantly independent forms of AMPA receptor-mediated excitation. The existence of direct glutamatergic transmission between mitral cells (which we will now refer to as chemical lateral excitation, LE), suggests that it might serve a functional role in glomerular processing rather then being an epiphenomenon of SE.

Chemical lateral excitation is modulated by sniffing-relevant patterns of activity

What might be the role of chemical LE within glomerular networks? Sniffing behaviour in rodents is known to alter during odour sampling (Kay & Laurent, 1999) and even during odour expectation (Uchida & Mainen, 2003; Kepecs *et al.* 2006) indicating that the sniff itself might facilitate odour processing (Kepecs *et al.* 2006; Schaefer *et al.* 2006; Schaefer & Margrie, 2007). *In vivo,* mitral cell activity can lock to the sniff cycle that occurs in the theta frequency range (sniffing cycle ∼200 ms) whereby mitral cells tend to fire action potentials in bursts at approximately 50–60 Hz (Margrie & Schaefer, 2003). We therefore investigated the possibility that LE might be sensitive to the kinds of temporal patterning observed in the olfactory bulb during the sniff cycle.

To examine this question we used a theta-burst stimulation (TBS) protocol that approximates the sniff-related activity of mitral cells observed *in vivo*. TBS was found to potentiate LE at some connections while
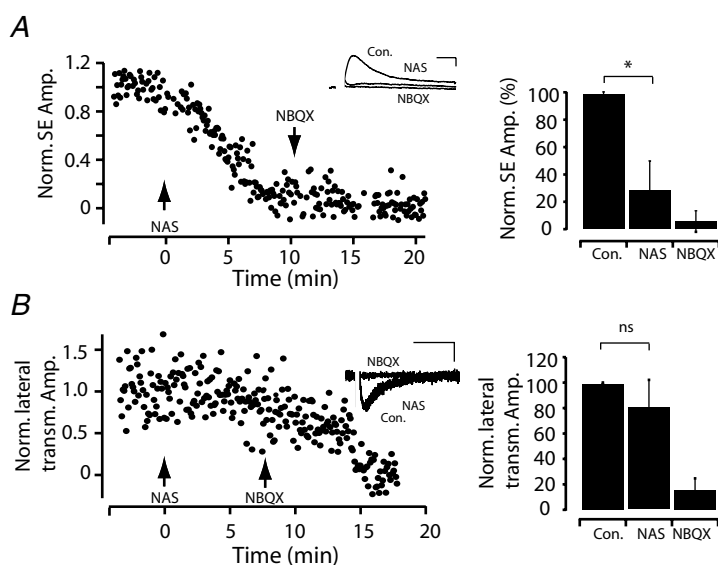

Figure 6. SE and lateral transmission are mediated by different subtypes of glutamate receptors
A, plot of the normalized SE amplitude over time. At $t = 0$ min the specific calcium-permeable AMPA receptor antagonist NAS (20 μM) was applied to the bath solution followed by application of NBQX (20 μM) at $t = 10$ min. Inset, example average traces recorded in current clamp (30 sweeps, scale bars represent 10 ms, 500 μV). Right, population data ($n = 8$) showing the effects of NAS and NBQX on SE. *B*, plot of the normalized amplitude of lateral transmission over time; arrows indicate the beginning of bath application of NAS and NBQX as in A. Inset, example traces recorded in voltage clamp (30 sweeps, scale bars represent 10 ms, 10 pA). Bar graphs (right) for population data ($n = 7$) showing the lack of sensitivity of lateral transmission to NAS (bars correspond to standard deviation).

depressing it at others (examples in Fig. 7*Aa*, *b* and *c*). Plotting the percentage amplitude change against the initial LE strength revealed a linear correlation whereby weak connections exhibit potentiation while larger connections undergo depression ($R^2 = 0.53$, $P < 0.01$; $n = 18$; Fig. 7*B*). Such changes in the amplitude and direction of plasticity were not associated with any modulation of electrical coupling ($P > 0.7$, $n = 14$).

To investigate the potential locus of the observed LE plasticity, in a subset of cells we first used a paired-pulse protocol that assays potential changes in the probability of transmitter release (Fatt & Katz, 1952; Zucker & Regehr, 2002). In all cases where this was examined TBS-induced changes in LE strength parallelled changes in the paired-pulse ratio ($R^2 = 0.91$, $P < 0.05$, Fig. 8*A*, $n = 5/5$) whereby increases in LE efficacy were associated with a decrease in the paired-pulse facilitation ratio and vice versa. To further assess the possibility that presynaptic mechanisms may be involved in LE plasticity, we determined whether a change in the coefficient of variation of LE also parallels the direction and amplitude of plasticity. Normalized CV^2/amplitude plots can provide

an indication of the locus of changes in synaptic efficacy whereby gradients steeper than unity are considered predominantly presynaptic (Malinow & Tsien, 1990; Faber & Korn, 1991; Hardingham *et al.* 2007). We find on average that the gradient of the ratiometric change in the coefficient of variation for both depression and potentiation is steeper than the unity line indicating a presynaptic component (Fig. 8*Ba* and *b*, respectively). Although several connections fell close to and some outside the presynaptic locus quadrant (see Fig. 8*B*) such cells often displayed large changes in EPSP variance in the predicted direction (for example see Fig. 7*Ab* and *c*) but rather the amplitude of the EPSP appeared to change to a lesser extent (example Figs 7*Ab* and *c*, and 8*Ba* and *b*). This together with our paired-pulse data suggest that a presynaptic mechanism is probably involved in LE plasticity within mitral cell assemblies.

Discussion

Here we show that within the glomerulus network under physiological conditions mitral cells communicate via
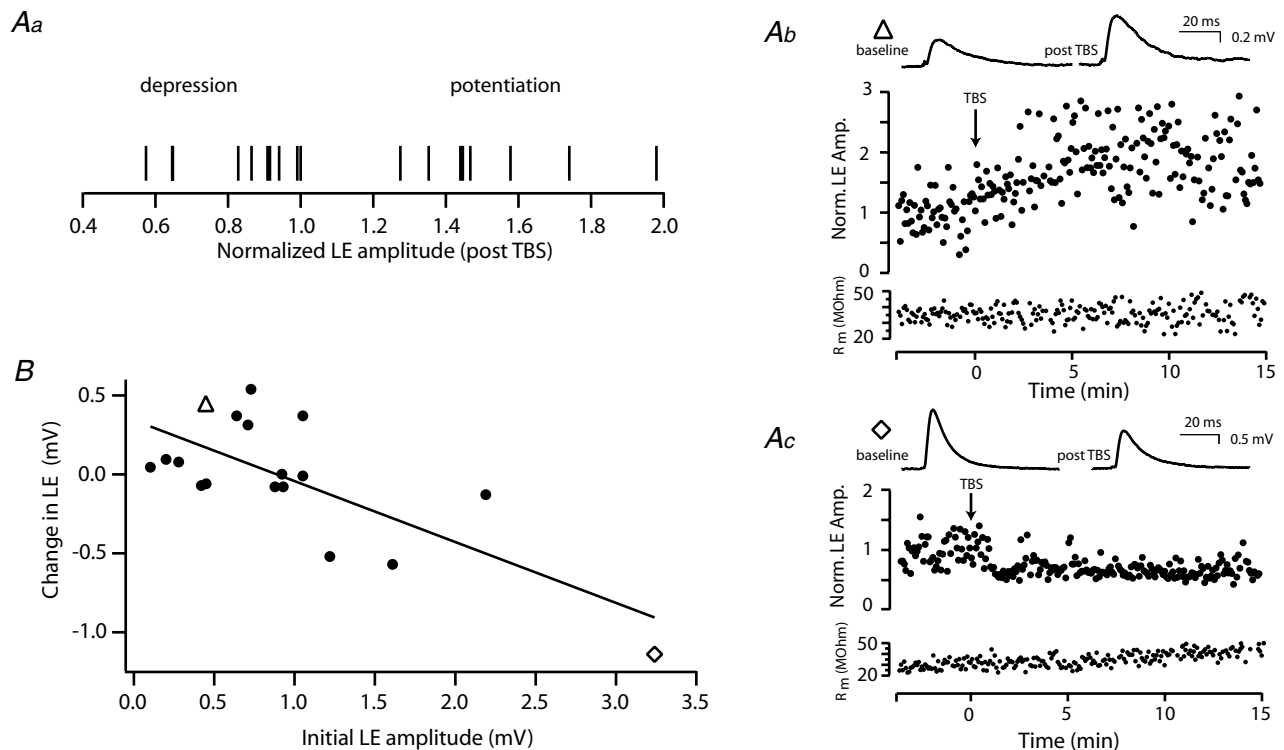

Figure 7. Chemical LE exhibits bi-directional plasticity
Aa, normalized change in LE amplitude for each connection. *Ab* and *Ac*, plots of LE amplitude over time illustrating examples of potentiation (*Ab*) and depression (*Ac*) following theta-burst stimulation (onset of TBS indicated by the arrow). TBS consisted of 150 bursts of 5 APs at 50 Hz repeated at 5 Hz (750 APs, total duration 30 s). Average traces (top) of 30 sweeps recorded in current clamp during the baseline and following TBS. Below is a plot of input resistance measured over time using a somatic hyperpolarizing pulse. *B*, population data showing the relationship between the initial LE amplitude and the observed absolute change in amplitude ($R^2 = 0.53$, $P < 0.01$ $n = 18$; △, connection shown in *Ab*; ◇, connection in *Ac*).

electrical and chemical transmission. Our data show that while self-excitation and electrical coupling are robust and reliable hallmarks of mitral cells, together they do not account for the reliability and strength of lateral transmission.

The most direct evidence that LE is an independent form of mitral cell communication comes from the observation that SE and LE rely on the activation of different types of AMPA receptors. While SE is mediated by calcium-permeable AMPA receptors, LE shows little sensitivity to a specific antagonist (NAS) for these receptors. Recently, calcium-permeable AMPA receptors have been shown to be crucial in some forms of synaptic plasticity (Cull-Candy *et al.* 2006) and in the retina, where expressed presynaptically, they can mediate transmitter release (Chavez *et al.* 2006). The fact that LE was found to be largely insensitive to NAS suggests that calcium-permeable AMPA receptors here are involved neither in LE release nor reception within intraglomerular mitral cell dendrites.

Our morphometric analysis of mitral cell pairs indicates that macroscopic features of tuft anatomy do not explain the likelihood of LE between a given cell pair. This may be indicative of several features of LE. Firstly, the connectivity rules for chemical LE might not follow that of electrical coupling and that LE may be more compartmentalized within the glomerulus. Alternatively all mitral cells belonging to the same glomerulus might well be chemically coupled and the cases of no apparent LE reflect dendritic filtering by the tuft and apical dendrite of comparatively small or more distant LE (Urban & Sakmann, 2002).

The fact that we only observe LE between mitral cells that project to the same glomerulus suggests that its locus is in the apical tuft. A third possibility, however, is that LE between mitral cell glomerular assemblies occurs, for example, in the lateral dendrites. In this scenario, lateral dendrites of cells belonging to the same glomerulus may more likely be closely apposed to another and thus more receptive to released glutamate. Recordings from mitral cells that project to different glomeruli, under conditions that enhance release and/or prevent reuptake or increase NMDA channel open probability, indicate that large depolarizing voltage steps can evoke glutamate spillover mediated by NMDA receptors in the lateral dendrite of other mitral cells (Isaacson, 1999; Christie & Westbrook, 2006). Although immunohistochemical evidence indicates that AMPA receptors reside along
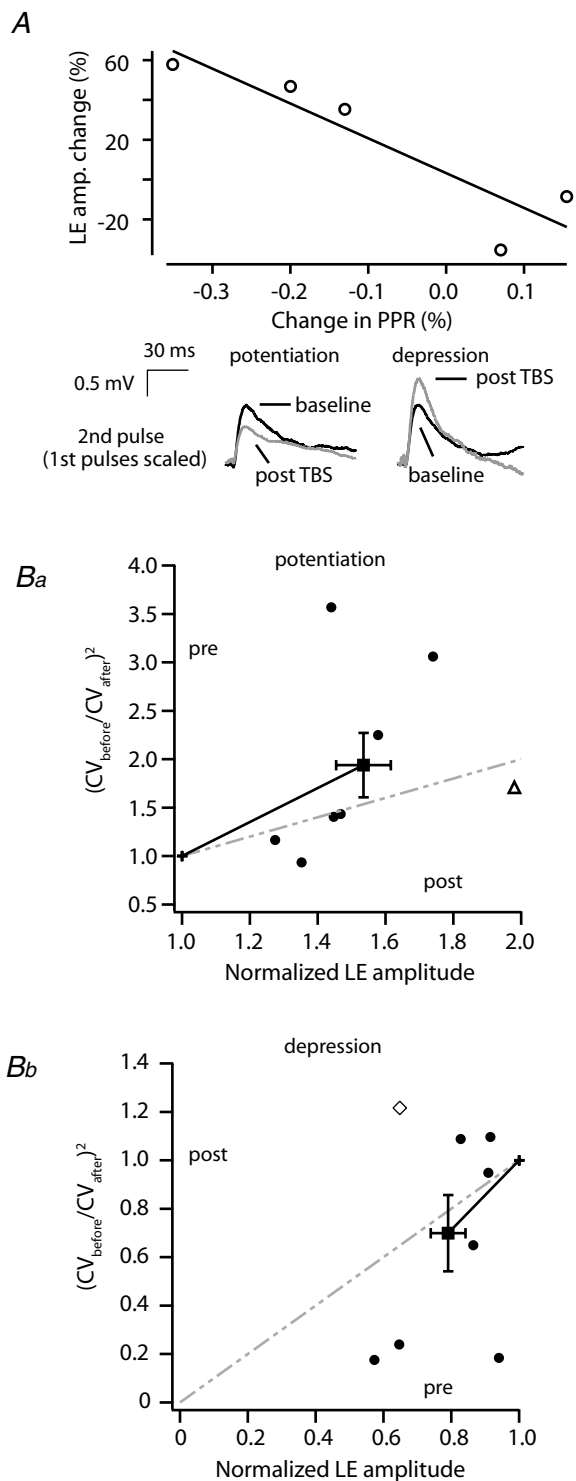
Figure 8. Induction of LE plasticity is associated with a change in dendritic release
A, a plot of the change in paired-pulse ratio (PPR) as it relates to changes in LE induced by TBS. Pairs of APs delivered at 20 Hz were used to evoke EPSPs in the second cell. The amplitude of the second EPSP was divided by the first and normalized over the baseline period (data from 5/5 pairs in which PPR was monitored). Below, average traces of the second EPSP (30 sweeps) recorded during the baseline period and following potentiation (left) and depression (right). The

amplitude of the first EPSP is scaled (not shown) to highlight the change in PPR. *B,* the change in the coefficient of variation (CV) following TBS plotted against post-TBS LE amplitude for potentiation (*Ba*) and depression (*Bb*) ($\triangle$, connection shown in Fig. 7*Ab*; $\diamond$, connection in Fig. 7*Ac*; bars represent standard error).

lateral dendrites (Montague & Greer, 1999), other studies suggest that AMPA receptors in the external plexiform layer are expressed exclusively in granule cell dendrites (Sassoe-Pognetto & Ottersen, 2000). To date, this purely NMDA receptor-mediated form of lateral communication is believed to be occurring via mitral cell lateral dendrites (Isaacson, 1999; Christie & Westbrook, 2006).

We have several lines of evidence that suggest the glutamatergic LE decribed here is not mediated via lateral dendrites. Under more physiological conditions single action potentials have been shown to propagate poorly into lateral dendrites (Margrie *et al.* 2001; Lowe, 2002; Christie & Westbrook, 2003) and thus far have not been shown to evoke NMDA-mediated spillover (Christie & Westbrook, 2006). Our experiments show that single action potentials are capable of evoking large EPSPs (greater than 2 mV) that are abolished by AMPA receptor antagonists. Thus, under physiological conditions that do not promote glutamate release and reception, we observe mitral cell–mitral cell transmission that is not indicative of spillover mediated exclusively by NMDA receptors in lateral or apical dendrites. Further evidence for a glomerular locus of chemical LE comes from previous recordings along the apical dendrite during 'presynaptic' stimulation of a paired mitral cell (Urban & Sakmann, 2002). Such data show that single action potential-evoked AMPA-mediated events occur earlier and are larger in the distal apical dendrite than those recorded at the soma. Our anatomical data extend this idea since we do not observe LE in cases where the apical tuft of one mitral cell is amputated but otherwise dendritically in close proximity to the other. Furthermore, LE was observed in pairs where the lateral dendrites appear not to closely oppose one another. Taken together it is therefore likely that AMPA receptor-mediated chemical LE is exclusively a glomerulus-based phenomenon.

The observation that LE is heterogeneously expressed, independently of the overall size of mitral cell tufts, suggests that the specification of these connections may be dependent on developmental features and/or history of activity, the rules for which remain undetermined. In order to identify the precise anatomical substrates for LE, quantification beyond light microscopy resolution will be necessary. Given the number of mitral cells per glomerulus and their elaborate tuft morphologies, ultrastructural analysis of entire glomeruli would ideally be required (Denk & Horstmann, 2004).

To date lateral transmission between mitral cells has previously been suggested to rely solely on gap junction-mediated transfer of SE (Schoppa & Westbrook, 2002; Christie *et al.* 2005). The direct evidence for this comes from a lack of lateral transmission observed in connexin36 knockout mice (Schoppa & Westbrook, 2002; Christie *et al.* 2005; Christie & Westbrook, 2006). Rather than a knockout approach we have used a correlation-based approach to examine any relation between SE, electrical coupling and LE. Together these data suggest that while gap junction-mediated coupling may be a requirement for the development of chemical LE, the degree of coupling does not determine the efficacy of LE. Such studies in connexin36 knockout mice further show that chemical transmission between mitral cell pairs can only occur during periods of high frequency activity in the presence of glutamate uptake blockers (Christie & Westbrook, 2006). In contrast, we find that under physiological conditions LE can be evoked by a single action potential, does not require artificially high concentrations of glutamate, and is therefore likely to contribute to intra-glomerular processing.

Gap junctions provide cells with electrical coupling via membrane pores that allow the flux of ions and even metabolites. Ionic flow is linear, bi-directional and can be of either polarity (Sohl *et al.* 2005). In mitral cells, depending on the time course and membrane potential, it is expected that inhibition, excitatory sensory drive and SE will propagate equally efficiently through such electrical synapses. This way electrical coupling could co-ordinate excitation and inhibition across connected cells, facilitating the synchronization of activity within the entire assembly (Bennett & Zukin, 2004). In contrast to gap junctions that do not discriminate in their transmission, chemical LE provides an exclusive excitatory pathway within the mitral cell network. Despite the fact that LE evoked by a single AP is typically modest in amplitude when measured at the soma, when evoked by several synchronous mitral cells it will substantially depolarize the postsynaptic cell. This is even more probable when considering that large-amplitude subthreshold oscillations are likely to further co-ordinate mitral activity around very depolarized membrane potentials *in vivo* (Luo & Katz, 2001; Cang & Isaacson, 2003; Margrie & Schaefer, 2003; Schaefer *et al.* 2006).

It is well known that dendritic release can be modulated by neuromodulators (Isaacson & Vitten, 2003; Davison *et al.* 2004) and high-frequency bursts of activity (Wilson & Nicoll, 2002; Freund *et al.* 2003). Here we show that in mitral cells, bursts of action potentials in the theta frequency range can regulate intraglomerular dendritic transmission. The sensitivity of LE to sniffing-like patterns of activity suggests that the efficacy of LE will be modulated under physiological conditions *in vivo* (Margrie & Schaefer, 2003; Schaefer *et al.* 2006; Schaefer & Margrie, 2007; Verhagen *et al.* 2007). In slices, theta-burst stimulation could induce changes in LE efficacy such that small connections were potentiated while larger connections showed depression. Recent work in layer 2/3 neocortical pyramidal cells show similarly that the initial strength of axo-dendritic connections can determine the direction and the amount of change in efficacy in a manner that is dependent on release probability (Hardingham

et al. 2007). Consistent with these findings, we observe that the direction and amplitude of plasticity correlates with changes in the paired-pulse ratio. As with layer 2/3 neurons, changes in the CV before and after induction of plasticity further indicate a presynaptic contribution.

To date the major form of plasticity within the bulb relies on neurogenesis whereby new interneurons are continuously integrated into the bulb circuitry over the time course of several weeks (Lledo *et al.* 2006). Our data show that instantaneous forms of dendro-dendritic plasticity also exist. One idea is that LE could provide a mechanism to change the gain function of an individual cell to match the overall glomerular input. This may act to compensate for flux in the ongoing degeneration and genesis of the sensory input that an individual mitral cell receives. In this manner, LE plasticity could serve to normalize sensitivity and provide reliable sensory reception and transmission at the level of the intra-glomerular mitral cell network. Such network homeostasis mechanisms would ensure that output from those cells belonging to the same functional assembly provide similar output patterns to different target cell populations in downstream structures (Suzuki & Bekkers, 2006).

References

Aungst JL, Heyward PM, Puche AC, Karnup SV, Hayar A, Szabo G & Shipley MT (2003). Centre-surround inhibition among olfactory bulb glomeruli. *Nature* **426**, 623–629.

Bekkers JM & Hausser M (2007). Targeted dendrotomy reveals active and passive contributions of the dendritic tree to synaptic integration and neuronal output. *Proc Natl Acad Sci U S A* **104**, 11447–11452.

Bennett MV & Zukin RS (2004). Electrical coupling and neuronal synchronization in the mammalian brain. *Neuron* **41**, 495–511.

Blakemore LJ, Resasco M, Mercado MA & Trombley PQ (2006). Evidence for Ca^{2+}-permeable AMPA receptors in the olfactory bulb. *Am J Physiol Cell Physiol* **290**, C925–C935.

Cang J & Isaacson JS (2003). In vivo whole-cell recording of odor-evoked synaptic transmission in the rat olfactory bulb. *J Neurosci* **23**, 4108–4116.

Chavez AE, Singer JH & Diamond JS (2006). Fast neurotransmitter release triggered by Ca influx through AMPA-type glutamate receptors. *Nature* **443**, 705–708.

Christie JM, Bark C, Hormuzdi SG, Helbig I, Monyer H & Westbrook GL (2005). Connexin36 mediates spike synchrony in olfactory bulb glomeruli. *Neuron* **46**, 761–772.

Christie JM & Westbrook GL (2003). Regulation of backpropagating action potentials in mitral cell lateral dendrites by A-type potassium currents. *J Neurophysiol* **89**, 2466–2472.

Christie JM & Westbrook GL (2006). Lateral excitation within the olfactory bulb. *J Neurosci* **26**, 2269–2277.

Cull-Candy S, Kelly L & Farrant M (2006). Regulation of Ca^{2+}-permeable AMPA receptors: synaptic plasticity and beyond. *Curr Opin Neurobiol* **16**, 288–297.

Davison IG, Boyd JD & Delaney KR (2004). Dopamine inhibits mitral/tufted → granule cell synapses in the frog olfactory bulb. *J Neurosci* **24**, 8057–8067.

Denk W & Horstmann H (2004). Serial block-face scanning electron microscopy to reconstruct three-dimensional tissue nanostructure. *PLoS Biol* **2**, e329.

Faber DS & Korn H (1991). Applicability of the coefficient of variation method for analyzing synaptic plasticity. *Biophys J* **60**, 1288–1294.

Fatt P & Katz B (1952). Spontaneous subthreshold activity at motor nerve endings. *J Physiol* **117**, 109–128.

Freund TF, Katona I & Piomelli D (2003). Role of endogenous cannabinoids in synaptic signaling. *Physiol Rev* **83**, 1017–1066.

Haberly LB & Price JL (1977). The axonal projection patterns of the mitral and tufted cells of the olfactory bulb in the rat. *Brain Res* **129**, 152–157.

Hardingham NR, Hardingham GE, Fox KD & Jack JJ (2007). Presynaptic efficacy directs normalization of synaptic strength in layer 2/3 rat neocortex after paired activity. *J Neurophysiol* **97**, 2965–2975.

Hayar A, Karnup S, Ennis M & Shipley MT (2004). External tufted cells: a major excitatory element that coordinates glomerular activity. *J Neurosci* **24**, 6676–6685.

Hayar A, Shipley MT & Ennis M (2005). Olfactory bulb external tufted cells are synchronized by multiple intraglomerular mechanisms. *J Neurosci* **25**, 8197–8208.

Horikawa K & Armstrong WE (1988). A versatile means of intracellular labeling: injection of biocytin and its detection with avidin conjugates. *J Neurosci Meth* **25**, 1–11.

Isaacson JS (1999). Glutamate spillover mediates excitatory transmission in the rat olfactory bulb. *Neuron* **23**, 377–384.

Isaacson JS & Vitten H (2003). $GABA_B$ receptors inhibit dendrodendritic transmission in the rat olfactory bulb. *J Neurosci* **23**, 2032–2039.

Jahr CE & Nicoll RA (1980). Dendrodendritic inhibition: demonstration with intracellular recording. *Science* **207**, 1473–1475.

Jahr CE & Nicoll RA (1982). An intracellular analysis of dendrodendritic inhibition in the turtle *in vitro* olfactory bulb. *J Physiol* **326**, 213–234.

Kaba H & Keverne EB (1988). The effect of microinfusions of drugs into the accessory olfactory bulb on the olfactory block to pregnancy. *Neuroscience* **25**, 1007–1011.

Karnup SV, Hayar A, Shipley MT & Kurnikova MG (2006). Spontaneous field potentials in the glomeruli of the olfactory bulb: the leading role of juxtaglomerular cells. *Neuroscience* **142**, 203–221.

Kay LM & Laurent G (1999). Odor- and context-dependent modulation of mitral cell activity in behaving rats. *Nat Neurosci* **2**, 1003–1009.

Kepecs A, Uchida N & Mainen ZF (2006). The sniff as a unit of olfactory processing. *Chem Senses* **31**, 167–179.

Kosaka T & Kosaka K (2005). Intraglomerular dendritic link connected by gap junctions and chemical synapses in the mouse main olfactory bulb: electron microscopic serial section analyses. *Neuroscience* **131**, 611–625.

Li Z (1990). A model of olfactory adaptation and sensitivity enhancement in the olfactory bulb. *Biol Cybern* **62**, 349–361.

Lledo PM, Alonso M & Grubb MS (2006). Adult neurogenesis and functional plasticity in neuronal circuits. *Nat Rev Neurosci* **7**, 179–193.

Lowe G (2002). Inhibition of backpropagating action potentials in mitral cell secondary dendrites. *J Neurophysiol* **88**, 64–85.

Luo M & Katz LC (2001). Response correlation maps of neurons in the mammalian olfactory bulb. *Neuron* **32**, 1165–1179.

Ma J & Lowe G (2007). Calcium permeable AMPA receptors and autoreceptors in external tufted cells of rat olfactory bulb. *Neuroscience* **144**, 1094–1108.

Malinow R & Tsien RW (1990). Presynaptic enhancement shown by whole-cell recordings of long-term potentiation in hippocampal slices. *Nature* **346**, 177–180.

Margrie TW, Sakmann B & Urban NN (2001). Action potential propagation in mitral cell lateral dendrites is decremental and controls recurrent and lateral inhibition in the mammalian olfactory bulb. *Proc Natl Acad Sci U S A* **98**, 319–324.

Margrie TW & Schaefer AT (2003). Theta oscillation coupled spike latencies yield computational vigour in a mammalian sensory system. *J Physiol* **546**, 363–374.

Montague AA & Greer CA (1999). Differential distribution of ionotropic glutamate receptor subunits in the rat olfactory bulb. *J Comp Neurol* **405**, 233–246.

Mori K, Kishi K & Ojima H (1983). Distribution of dendrites of mitral, displaced mitral, tufted, and granule cells in the rabbit olfactory bulb. *J Comp Neurol* **219**, 339–355.

Murphy GJ, Darcy DP & Isaacson JS (2005). Intraglomerular inhibition: signaling mechanisms of an olfactory microcircuit. *Nat Neurosci* **8**, 354–364.

Nagayama S, Takahashi YK, Yoshihara Y & Mori K (2004). Mitral and tufted cells differ in the decoding manner of odor maps in the rat olfactory bulb. *J Neurophysiol* **91**, 2532–2540.

Nicoll RA & Jahr CE (1982). Self-excitation of olfactory bulb neurones. *Nature* **296**, 441–444.

Pinching AJ & Powell TP (1971*a*). The neuron types of the glomerular layer of the olfactory bulb. *J Cell Sci* **9**, 305–345.

Pinching AJ & Powell TP (1971*b*). The neuropil of the glomeruli of the olfactory bulb. *J Cell Sci* **9**, 347–377.

Price JL & Powell TP (1970). The mitral and short axon cells of the olfactory bulb. *J Cell Sci* **7**, 631–651.

Rall W, Shepherd GM, Reese TS & Brightman MW (1966). Dendrodendritic synaptic pathway for inhibition in the olfactory bulb. *Exp Neurol* **14**, 44–56.

Rosser AE & Keverne EB (1985). The importance of central noradrenergic neurones in the formation of an olfactory memory in the prevention of pregnancy block. *Neuroscience* **15**, 1141–1147.

Salin PA, Lledo PM, Vincent JD & Charpak S (2001). Dendritic glutamate autoreceptors modulate signal processing in rat mitral cells. *J Neurophysiol* **85**, 1275–1282.

Sassoe-Pognetto M & Ottersen OP (2000). Organization of ionotropic glutamate receptors at dendrodendritic synapses in the rat olfactory bulb. *J Neurosci* **20**, 2192–2201.

Schaefer AT, Angelo K, Spors H & Margrie TW (2006). Neuronal oscillations enhance stimulus discrimination by ensuring action potential precision. *PLoS Biol* **4**, e163.

Schaefer AT & Margrie TW (2007). Spatiotemporal representations in the olfactory system. *Trends Neurosci* **30**, 92–100.

Schoppa NE & Westbrook GL (2001). Glomerulus-specific synchronization of mitral cells in the olfactory bulb. *Neuron* **31**, 639–651.

Schoppa NE & Westbrook GL (2002). AMPA autoreceptors drive correlated spiking in olfactory bulb glomeruli. *Nat Neurosci* **5**, 1194–1202.

Sohl G, Maxeiner S & Willecke K (2005). Expression and functions of neuronal gap junctions. *Nat Rev Neurosci* **6**, 191–200.

Sullivan RM, Stackenwalt G, Nasr F, Lemon C & Wilson DA (2000). Association of an odor with activation of olfactory bulb noradrenergic β-receptors or locus coeruleus stimulation is sufficient to produce learned approach responses to that odor in neonatal rats. *Behav Neurosci* **114**, 957–962.

Suzuki N & Bekkers JM (2006). Neural coding by two classes of principal cells in the mouse piriform cortex. *J Neurosci* **26**, 11938–11947.

Uchida N & Mainen ZF (2003). Speed and accuracy of olfactory discrimination in the rat. *Nat Neurosci* **6**, 1224–1229.

Urban NN & Sakmann B (2002). Reciprocal intraglomerular excitation and intra- and interglomerular lateral inhibition between mouse olfactory bulb mitral cells. *J Physiol* **542**, 355–367.

Verhagen JV, Wesson DW, Netoff TI, White JA & Wachowiak M (2007). Sniffing controls an adaptive filter of sensory input to the olfactory bulb. *Nat Neurosci* **10**, 631–639.

Wilson DA, Fletcher ML & Sullivan RM (2004). Acetylcholine and olfactory perceptual learning. *Learn Mem* **11**, 28–34.

Wilson RI & Nicoll RA (2002). Endocannabinoid signaling in the brain. *Science* **296**, 678–682.

Zucker RS & Regehr WG (2002). Short-term synaptic plasticity. *Annu Rev Physiol* **64**, 355–405.

Acknowledgements